Chapter 2
Thermodynamic Concepts—Equilibrium and Nonequilibrium During Solidification

Thermodynamics is a useful tool for the analysis of solidification. It is used to evaluate alloy phase constitution, the solidification path, basic alloy properties such as partition coefficients, slopes of liquidus, and solidus phase boundaries.

2.1 Equilibrium

The free energy of any phase is a function of pressure, temperature, and composition. Equilibrium is attained when the Gibbs free energy is at a minimum (equivalent to mechanical systems for which equilibrium exists when the potential energy is at a minimum). Thus the condition is:

$$dG(P, T, n_i \ldots) = \left(\frac{\partial G}{\partial T}\right)_{P,n_i\ldots} dT + \left(\frac{\partial G}{\partial P}\right)_{T,n_i\ldots} dP + \left(\frac{\partial G}{\partial n_i}\right)_{T,P,n_j\ldots} dn_i + \ldots = 0 \tag{2.1}$$

where n_i is the number of moles (or atoms) of component i. The partial derivatives of the free energy are called partial molar free energies, or *chemical potentials*:

$$\mu_i = \left(\frac{\partial G}{\partial n_i}\right)_{T,P,n_j,\ldots} \tag{2.2}$$

At equilibrium, and assuming T, P = constant,

$$dG = \mu_i dn_i + \mu_j dn_j + \ldots = 0 \tag{2.3}$$

For a multiphase system, a condition for equilibrium is that the chemical potential of each component must be the same in all phases (for derivation see inset):

$$\mu_i^{\alpha} = \mu_i^{\beta} \tag{2.4}$$

where the superscripts and β stand for the two phases.

D. M. Stefanescu, *Science and Engineering of Casting Solidification,*
DOI 10.1007/978-3-319-15693-4_2

Derivation of the Equilibrium Criterion

Consider two phases, α and β, within a system at equilibrium. If an amount of dn of component A is transferred from phase α to phase β at T, $P = ct.$, the change in free energy associated with each phase is $dG^{\alpha} = \mu_A^{\alpha} dn$ and $dG^{\beta} = -\mu_A^{\beta} dn$. The total change in free energy is $dG = dG^{\alpha} + dG^{\beta} = (\mu_A^{\alpha} - \mu_A^{\beta})dn$.

Since at equilibrium $dG = 0$, it follows that $\mu_A^{\alpha} - \mu_A^{\beta} = 0$.

Although equilibrium conditions do not actually exist in real systems, under the assumption of *local thermodynamic equilibrium*, the liquid and solid composition of metallic alloys can be determined using *equilibrium phase diagrams*. Local equilibrium implies that reaction rates at the solid/liquid interface are rapid when compared to the rate of interface advance. This concept has been shown experimentally to be true up to the solidification velocities of 5 m/s.

Equilibrium phase diagrams describe the structure of a system as a function of composition and temperature, assuming transformation rate is extremely slow, or species diffusion rate is very fast. Two-component phase equilibrium in a binary system occurs when the chemical potentials of the two species are equal.

Phase diagrams were originally obtained from experimental cooling curves. The progress in thermodynamics and computational thermodynamics developed the method of constructing phase diagrams with the help of the Gibbs free energy curves. A simple example for the case of nonideal solution is given in Fig. 2.1. G_m is the Gibbs free energy of mixing, which for nonideal binary solutions is given by:

$$G_m = x_A G_A^o + x_B G_B^o + RT(x_A \ln x_A + x_B \ln x_B) + G_m^{Ex} \tag{2.5}$$

where

x	Molar faction of components A or B
G^o	Free energy of the pure component A or B
R	Gas constant
	$G_m^{Ex} = G_m^{non-ideal} - G_m^{ideal} = H_m^{mix}(1 - AT)$ Excess free energy
A	Constant to be evaluated through experiments

In Fig. 2.1, at temperature T_1, the energy of the liquid, G_m^L, is smaller than that of the solid, G_m^S, and the liquid phase is the stable phase at all compositions. At temperature $T_2 < T_1$, the free energy curves intersect. A tangent to the two curves gives the region where the two phases, L and α-solid, coexist. At temperature $T_3 < T_2$, the tangent construction produces two two-phase regions, L + α and L + β. At temperature T_4, the tangent is in contact with the three phases, L, α, and β, corresponding to a triple point, which is the eutectic point on the phase diagram. At temperature T_5, G_m^L is above the tangent, which means that there is no liquid. The central region is a mixture of the two phases α and β.

For an in-depth discussion of the thermodynamics of solidification the reader is referred to Fredriksson and Åkerlind (2012).

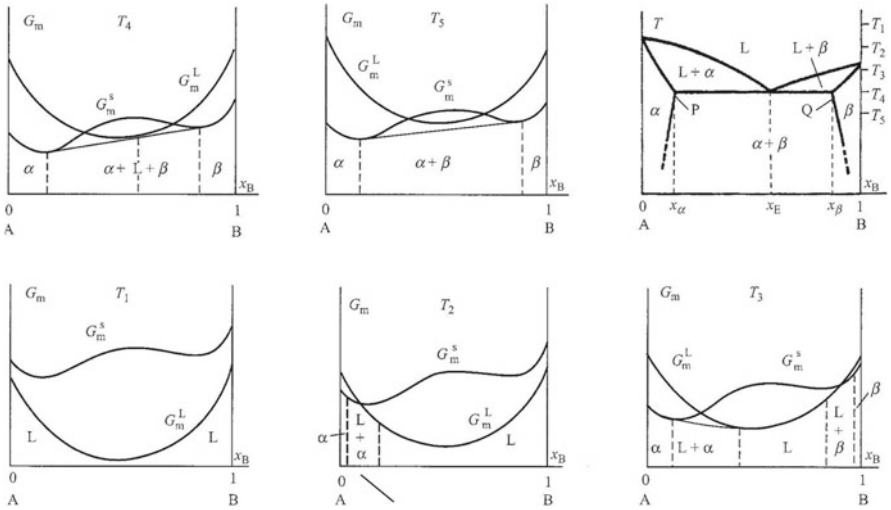

Fig. 2.1 Use of Gibbs free energy curves to calculate a binary phase diagram (Fredriksson and Åkerlind 2012). With permission from Wiley

2.2 The Undercooling Requirement

The driving force of any phase transformation including solidification, which is a liquid-to-solid phase transformation, is the change in free energy. The Helmholtz free energy per mole (molar free energy) or per unit volume (volumetric free energy) of a substance can be expressed as:

$$F = E + P \cdot v - T \cdot S \tag{2.6}$$

E Internal energy, i.e., the amount of work required to separate the atoms of the phase to infinity
P Pressure
v Volume
T Temperature
S Entropy

Thermodynamics stipulates that in a system without outside intervention, the free energy can only decrease.

The entropy is a measure of the amount of disorder in the arrangement of atoms in a phase. In the solid phase, the disorder results from the thermal vibrations of the atoms around their equilibrium position at lattice points. In the liquid phase, additional disorder comes from structural disorder, since the atoms do not occupy all the positions in the lattice as they do in solids. Indeed, the greater thermal energy at higher temperatures introduces not only greater thermal vibrations but also vacancies. Immediately below its melting point a metal may contain 0.1 % vacancies in its

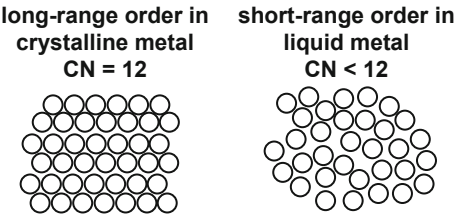

Fig. 2.2 Schematic representation of long- and short-range order regions (solid and liquid metals, respectively)

lattice. When the vacancies approach 1 % in a closed-packed structure, the regular 12-fold coordination is destroyed and the long-range order of the crystal structure disappears. The number of nearest neighbors decreases from 12 to 11 or even 10 (the coordination number (CN), becomes smaller than 12, as shown in Fig. 2.2). The pattern becomes irregular and the space per atom and the average interatomic distance are increased. Short-range order is instated. In other words, the liquid possesses a larger degree of disorder than the solid. Thus, the entropy of the liquid is higher than the entropy of the solid. The disorder resulting from melting increases the volume of most materials.

A certain amount of heat, the heat of fusion, is required to melt a specific material. Since the heat of fusion is the energy required to disorganize a mole of atoms, and the melting temperature is a measure of the atomic bond strength, there is a direct correlation between the two.

Let us start our analysis of solidification by introducing a number of simplifying assumptions:

a. Pure metal
b. Constant pressure
c. Flat solid/liquid interface, i.e., the radius of curvature of the interface is $r = \infty$
d. No thermal gradient in the liquid.

For constant pressure, Eq. 2.6 becomes the Gibbs free energy equation:

$$G = H - TS \tag{2.7}$$

where $H = E + P \cdot v$ is the enthalpy.

Eq. 2.7 is plotted in Fig. 2.3. Since the slope of the line corresponding to the liquid free energy is higher (i.e., $S_L > S_S$), the two lines must intersect at a temperature $T_{e\alpha}$. This is the equilibrium temperature at which no transformation (melting on heating or solidification on cooling) can occur. Under normal nucleation conditions, when the temperature decreases under $T_{e\alpha}$, α-stable solid will form. If nucleation of α is suppressed, β-metastable solid will form at a lower temperature, under $T_{e\beta}$. If nucleation of both α and β is suppressed, then metastable glass forms. The metastable γ solid can only be produced by vapor deposition.

The equilibrium condition Eq. 2.4 can be written for the case of solidification as:

$$\mu_L - \mu_S = 0 \quad \text{or} \quad G_L - G_S = 0 \tag{2.8}$$

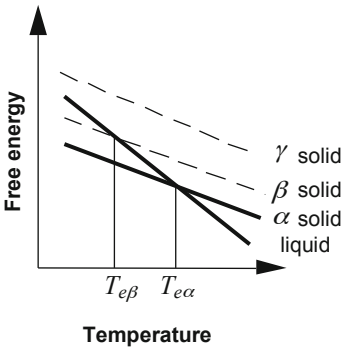

Fig. 2.3 Variation of the free energy of the liquid and solid with temperature

where the subscripts L and S stand for liquid and solid, respectively. This means that at equilibrium the change in chemical potential or in free energy is zero. At the equilibrium temperature, if the two phases coexist:

$$\Delta G_v = G_L - G_S = (H_L - H_S) - T_e(S_L - S_S) = 0$$

Thus, one can further write:

$$\Delta H_f = T_e \Delta S_f \quad \text{or} \quad \Delta S_f = \Delta H_f / T_e$$

Here, $\Delta H_f = H_L - H_S$ is the change in enthalpy during melting, or the volumetric latent heat. ΔS_f is the entropy of fusion (melting). At a temperature lower than T_e:

$$\Delta G_v = \Delta H_f - T\frac{\Delta H_f}{T_e} = \Delta H_f \frac{T_e - T}{T_e} = \Delta S_f \Delta T \tag{2.9}$$

ΔT is the undercooling at which the liquid-to-solid transformation occurs. From this equation the undercooling is defined as:

$$\Delta T = \Delta G_v / \Delta S_f \tag{2.10}$$

Note that if $\Delta T = 0$, $\Delta G_v = 0$. This means that, if there is no undercooling under the equilibrium temperature, the system is at equilibrium, and no transformation can occur.

Thermodynamics does not allow further clarification of the nature of undercooling. It simply demonstrates that undercooling is necessary for solidification to occur. Kinetics considerations must be introduced to further understand this phenomenon.

This analysis has been conducted under the four simplifying assumptions (*a*–*d*) previously listed. The analysis states that the only change in free energy upon solidification is because of the change of a volume of liquid into a solid, ΔG_v. However, when the four assumptions are relaxed the system will increase its free energy. This increase can be described by the sum of the increases resulting from the relaxation of each particular assumption:

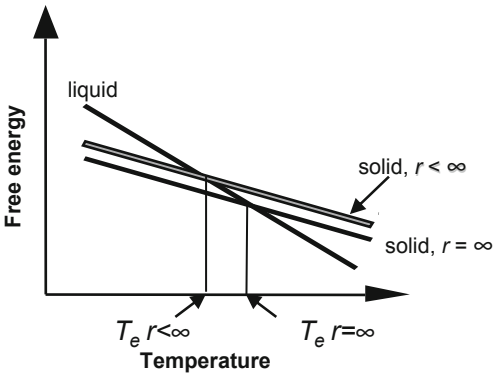

Fig. 2.4 Decrease of equilibrium temperature because of the curvature of the S/L interface

$$\Delta F = -\Delta G_v + \Delta G_r + \Delta G_T + \Delta G_c + \Delta F_P \tag{2.11}$$

The four positive right hand terms are the increase in free energy because of curvature, temperature, composition, and pressure variation, respectively. Let us now evaluate the terms in this equation.

2.2.1 Curvature Undercooling

In the evaluation of the equilibrium temperature presented so far, it has been assumed that the liquid–solid interface is planar (flat), i.e., of infinite radius (assumption c). This is seldom the case in real processes, and never the case at the beginning of solidification, because solidification is initiated at discrete points (nuclei) in the liquid, or at the walls of the mold that contains the liquid. As the volume of a solid particle in a liquid decreases, its surface/volume ratio increases and the contribution of the interface energy to the total free enthalpy of the particle increases. Thus, when the particle size decreases in a liquid–solid system, the total free enthalpy of the solid increases. The curve describing the free energy of the solid in Fig. 2.3 is moved upward by ΔG_r. This results in a decrease of the melting point (equilibrium temperature) as shown in Fig. 2.4.

If solidification begins at a point in the liquid, a spherical particle is assumed to grow in the liquid, and an additional free energy associated with the additional interface, different than ΔG_v, must be considered. This additional energy results from the formation of a new interface and is a function the curvature of the interface.

In two dimensions, the curvature of a function is the change in slope, $\delta\theta$, over a length of arc, δl, (Fig. 2.5):

$$K = \delta\theta/\delta l = \delta\theta/(r\delta\theta) = 1/r \tag{2.12}$$

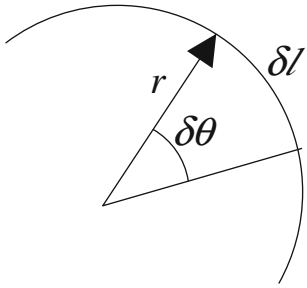

Fig. 2.5 Definition of curvature

In three dimensions, the curvature is the variation in surface area divided by the corresponding variation in volume:

$$K = dA/dv = 1/r_1 + 1/r_2 \tag{2.13}$$

where r_1 and r_2 are the principal radii of curvature (minimum and maximum value for a given surface).

For a sphere $r_1 = r_2$ and thus $K = 2/r$
For a cylinder $r_1 = \infty, r_2 = r$ and thus $K = 1/r$.

General Definition of Curvature

In general, if a curve is represented by $\mathbf{r}(t)$, where t is any parameter, the curvature of that curve is:

$K(t) = \frac{\sqrt{(\mathbf{r}'\cdot\mathbf{r}')(\mathbf{r}''\cdot\mathbf{r}'')-(\mathbf{r}'\cdot\mathbf{r}'')^2}}{(\mathbf{r}'\cdot\mathbf{r}')^{3/2}}$ where $r = dr/dt$ and $r = d^2r/dt^2$. In Cartesian coordinates, for a curve $y = y(x)$:

$K(x) = \frac{|y''|}{(1+y'^2)^{3/2}}$ where $y = dy/dx$, etc.

Assuming that the radius of the spherical particle is r, when the particle increases by dr, the work resulting from the formation of a new surface, $d(4\pi r^2\gamma)/dr$, must be equal to that resulting from the decrease of the free volumetric energy, i.e., $\frac{d}{dr}\left(\frac{4}{3}\pi r^3 \Delta G_v\right)$. Equating the two, after differentiation, the increase in free energy is:

$$\Delta G_v = 2\gamma/r \quad \text{or, more general} \quad \Delta G_v = \gamma K \tag{2.14}$$

where

γ Liquid–solid surface energy
K Curvature

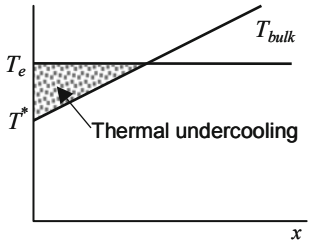

Fig. 2.6 Bulk thermal undercooling

Then, from the definition of undercooling, Eq. (2.9), we obtain:

$$\Delta S_f \Delta T_r = \gamma K \text{ or } \Delta T_r = T_e - T_e^r = \left(\gamma / \Delta S_f\right) K = \Gamma K \tag{2.15}$$

where ΔT_r is the curvature undercooling, T_e^r is the equilibrium (melting) temperature for a sphere of radius r, and Γ is the Gibbs–Thomson coefficient. The Gibbs–Thomson coefficient is a measure of the energy required to form a new surface (or expand an existing one). For most metals $\Gamma = 10^{-7}$ K m. In some calculations, molar ΔH_f and ΔS_f are used, for which the units are J mole^{-1} and J mole^{-1}K^{-1}, respectively. Then the Gibbs–Thomson coefficient becomes:

$$\Gamma = v_m \gamma / \Delta S_f \tag{2.16}$$

where v_m is the molar volume in m^3/mole.

For a spherical crystal $\Delta T_r = 2\ \Gamma/r$. Using this equation it follows that for $\Delta T_r = 2\,^\circ$C, $r = 0.1$ μm, and for $\Delta T_r = 0.2\,^\circ$C, $r = 1$ μm. Thus, the S/L interface energy is important only for morphologies where $r < 10$ μm, i.e., nuclei, interface perturbations, dendrites, and eutectic phases.

2.2.2 Thermal Undercooling

Let us now relax assumption (d), and allow a thermal gradient to exist in the liquid (Fig. 2.6). As long as nucleation of solid and subsequent growth of these nuclei is rather fast, the only S/L interface undercoolings for the pure metal are kinetic and curvature. However, if nucleation difficulties are encountered, or if growth of the solid lags heat transport out of the liquid, an additional undercooling, *thermal undercooling*, ΔT_T, occurs. When ignoring kinetic undercooling, this additional undercooling is simply the amount the liquid is under the equilibrium temperature of the pure metal solidifying with a planar interface (no curvature). Thus, the bulk thermal undercooling is:

$$\Delta T_T^{bulk} = T_e - T_{bulk} \tag{2.17}$$

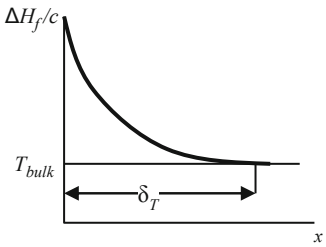

Fig. 2.7 Interface thermal undercooling

where T_{bulk} is the bulk liquid temperature (temperature far from the interface that can be measured through a thermocouple).

At the S/L interface the rejection of latent heat must also be considered. As shown in Fig. 2.7, a boundary layer of height $\Delta H_f/c$, and length δ_T will form at the interface (position $x = 0$), because of heat accumulation at the interface. The interface thermal undercooling can be calculated as:

$$\Delta T_T^* = T^* - T_{bulk} \tag{2.18}$$

The corresponding increase in free energy is $\Delta G_T = \Delta S_f(T^* - T_{bulk})$. Sometimes, metals can undercool considerably before solidifying. For example, pure iron can be undercooled under its melting (equilibrium) temperature by 300 °C, or even more, under certain controlled conditions.

2.2.3 Constitutional Undercooling

Up to this point, only pure metals have been considered (assumption a). For alloys, the solutal field introduces an additional change in the free energy, which corresponds to an additional undercooling. Fig. 2.8 shows the left corner of the phase diagram of a hypothetical alloy solidifying to form a single-phase solid solution. T_L is the liquidus temperature, T^* is the interface temperature at some arbitrary time during solidification, and T_S is the solidus temperature. Note that for alloys, T_L is the equilibrium temperature T_e. At temperature T^*, the composition of the solid at the interface is C_S^*, while the composition of the liquid is C_L^*. The bulk composition of the alloy, at the beginning of solidification, is C_o. The ratio between the solid composition and the liquid composition at the interface is called the *equilibrium partition coefficient*, k:

$$k = (C_S^*/C_L^*)_{T,P} \tag{2.19}$$

The indices T and P mean that calculations are made at constant temperature (isotherm) and at constant pressure (isobar). Note that at the end of solidification,

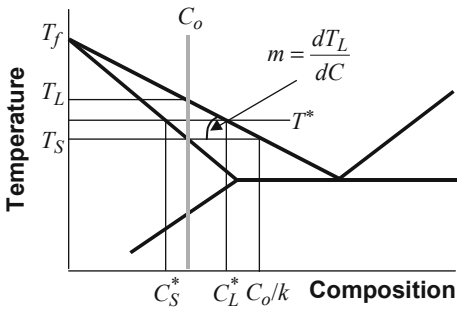

Fig. 2.8 Schematic region of a phase diagram for a solid solution alloy

T_S, it can be calculated that the last liquid to solidify should be of composition C_o/k. For the particular case described in Fig. 2.8, there is more solute in the liquid than in the solid at the interface. This partition is the cause of the occurrence of macrosegregation and microsegregation in alloys, to be discussed later in more detail.

The partition coefficient is constant only when the liquidus slope, m, is constant. Since for most of the alloys m is variable, so is k. Nevertheless, for mathematical simplicity, in most analytical calculations m and k are assumed constant. Note that $k < 1$ when the left-hand corner of a phase diagram is considered. However, $k > 1$ when the slopes of the liquidus and solidus lines are positive.

The following relationships exist between various temperatures and compositions in Fig. 2.8:

$$\Delta T_o = T_L - T_S = -m \cdot \Delta C_o \text{ and } \Delta C_o = C_o(1-k)/k \tag{2.20}$$

where ΔT_o is the liquidus–solidus temperature interval at C_o, and ΔC_o is the concentration difference between liquid and solid at T_S.

For dilute solutions, the Van't Hoff equation for liquid–solid equilibrium, $d(\ln k_e)/dT = \Delta H_f/RT^2$, holds and can be used to calculate k. Integrating between the melting temperature of solute B, T_f^B, and solvent A, T_f^A, gives:

$$k = \exp\left[\left(\Delta H_f^B/R\right)\left(1/T_f^B - 1/T_f^A\right)\right] \tag{2.21}$$

In addition, k and m relate as:

$$k = 1 - m\Delta H_f^A / \left[R\left(T_f^A\right)^2\right] \tag{2.22}$$

Here, ΔH_f^i is the latent heat of phase i, T_f^i is the melting temperature of phase i, and R is the gas constant. The index i stands for the pure solvent, A, or the solute, B.

The difference between the solid and liquid solubility of the alloying element is responsible for the occurrence of an additional undercooling called as *constitutional, or compositional, or solutal, undercooling* (ΔT_c). The concept was first introduced by Chalmers (1956). Consider the diagrams in Fig. 2.9. The first diagram in the

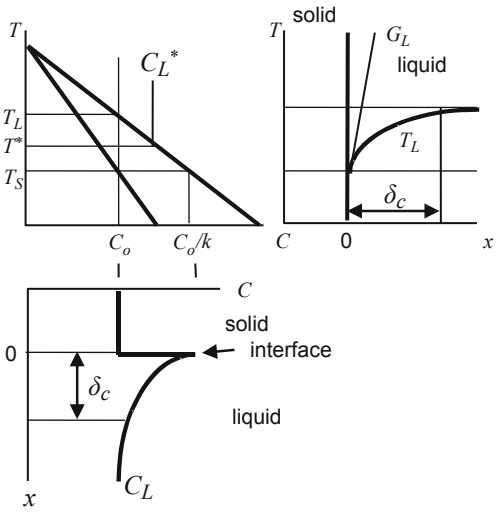

Fig. 2.9 The thermal and solutal field in front of the solid/liquid interface

upper left corner is a temperature—composition plot, that is, a phase diagram. C_o is the composition of the solid at temperature T_S, while C_o/k is the composition of the liquid at the same temperature. These compositions have been translated onto the lower diagram, which is a composition—distance (x) diagram. A diffusion boundary layer, δ_c, is shown on the diagram. This layer occurs because at the interface the composition of the liquid is higher (C_o/k) than farther away in the bulk liquid (C_o), and consequently, the composition of the liquid, C_L, decreases from the interface toward the liquid.

The third diagram, on the upper right, is a temperature–distance diagram. It shows that the liquidus temperature in the boundary layer is not constant, but increases from T_S at the interface, to T_L in the bulk liquid. This is a consequence of the change in composition, which varies from C_o/k (at temperature T_S) at the interface, to C_o (at temperature T_L) in the bulk liquid. A liquidus (solutal) temperature gradient, G_L, can now be defined as the derivative of the $T_L(x)$ curve with respect to x at the temperature of the interface, T^* (Fig. 2.10).

Since heat is flowing out from the liquid through the solid, there is also a thermal gradient in the liquid, G_T, which is determined by the evolution of the thermal field. The two gradients are compared in Fig. 2.10. If $G_L < G_T$, the temperature of the liquid ahead of the interface is above the liquidus temperature of the alloy. If on the contrary, $G_L > G_T$, over a certain distance ahead of the interface, the liquid will be at a temperature lower than its liquidus. Thus, while the bulk liquid may be at a temperature above its liquidus, the liquid at the interface may be at a temperature below its liquidus, because of the solute concentration in the diffusion layer. This liquid is constitutionally undercooled. The undercooling associated with this liquid is called *constitutional, or compositional, or solutal, undercooling,* ΔT_c. Based on Fig. 2.9 it can be calculated as:

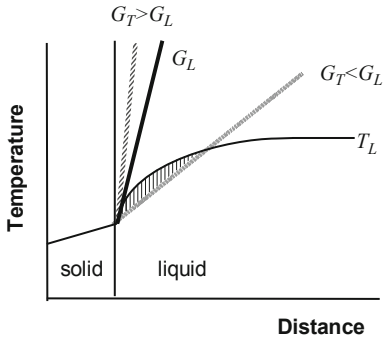

Fig. 2.10 Constitutional undercooling diagram comparing thermal (G_T) and liquidus (*compositional*) (G_L) gradients

$$\Delta T_c = T_L - T^* = -m(C_L^* - C_o) \tag{2.23}$$

Note that the sign convention here is that m is negative. The corresponding increase in free energy is:

$$\Delta G_c = -\Delta S_f m(C_L^* - C_o) \tag{2.24}$$

2.2.4 Pressure Undercooling

Let us now relax assumption (b) and consider that local pressure is applied on the S/L interface, or that pressure is applied on the whole system. The change in free energy of the liquid and solid with small changes in pressure and temperature can be calculated from Eq. 2.6 as:

$$\Delta F_L = v_L \Delta P - S_L \Delta T \text{ and } \Delta F_S = v_S \Delta P - S_S \Delta T$$

This is true assuming that the internal energy, the volume, and the entropy of the condensed matters (liquid and solid) change little under the proposed conditions. Then, from the equilibrium condition, $\Delta F_L = \Delta F_S$, the change in equilibrium temperature because of the applied pressure is:

$$\Delta T_P = \Delta P \Delta v / \Delta S_f \tag{2.25}$$

This equation is known as the Clapeyron equation. During solidification, the change in volume Δv is positive. Thus, an increase in pressure ($\Delta P > 0$) will result in an increase in undercooling.

For metals, the pressure undercooling is rather small, of the order of 10^{-2} K/atm. Hence, pressure-changes typical for usual processes have little influence on the melting temperature. However, in certain applications, such as particle engulfment by the S/L interface, the local pressure can reach relatively high values, and ΔT_P may become significant. Furthermore, starting again with Eq. 2.6, and using

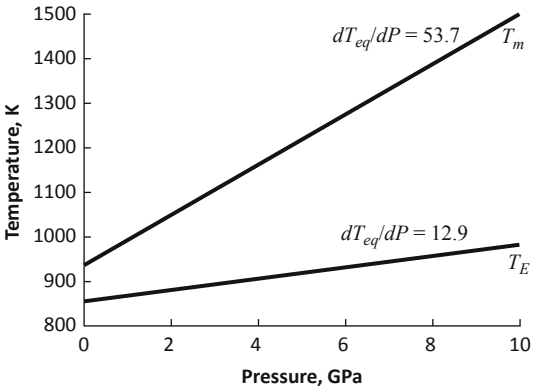

Fig. 2.11 Melting point of aluminum (T_m) and eutectic temperature of Al–Si system (T_E) as function of pressure (after Sobczak et al. 2012)

atoms in solid ⇒ *atoms in liquid*	melting
atoms in liquid ⇒ *atoms in solid*	solidification

differential notations, at constant temperature $dT = 0$, and the equation becomes $(\partial G/\partial P)_T = v$. This means that at constant temperature, the free energy of a phase increases with the increase in pressure, and a new phase with a smaller molar volume may form.

The Clapeyron equation also implies that a change in pressure will impose a change in the equilibrium temperature. Most metals and alloys expand upon melting so that in Eq. 2.25, $\Delta T_P/\Delta P > 0$. Consequently, a pressure increase will lead to an increase in melting temperature (see example in Fig. 2.11). Exceptions include Bi, Sb, Si, and graphitic cast iron, all of which expand upon solidification resulting in a decrease of the melting temperature.

For other effects of pressure on solidification phenomena the reader is referred to the review paper by Sobczak et al. (2012).

2.2.5 Kinetic Undercooling

The concept of undercooling can also be understood in terms of atom kinetics at the S/L interface. While this analysis is done at the atomic scale level, and a more in-depth discussion of this subject will be undertaken in Chapter 3, some concepts will be introduced here for clarity. When an S/L interface moves, the net transfer of atoms at the interface results from the difference between two atomic processes (Verhoeven 1975):

The rate of these two processes is:

$$\text{Rate of melting}\,(S \rightarrow L) = (dn/dt)_L = p_L n_S v_S \exp\left(-\Delta G_L/(k_B T)\right) \quad (2.26)$$

$$\text{Rate of solidification}\,(L \rightarrow S) = (dn/dt)_S = p_S n_L v_L \exp\left(-\Delta G_S/(k_B T)\right) \quad (2.27)$$

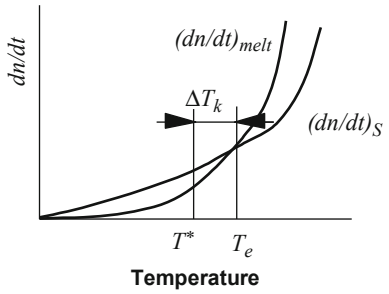

Fig. 2.12 Requirement of kinetic undercooling based on atomic kinetics considerations

where n_S, n_L are the number of atoms per unit area of solid and liquid interface respectively, ν_S, ν_L are the vibration frequencies of solid and liquid atoms, respectively, ΔG_{melt}, ΔG_S are the activation energy for an atom jumping through the interface during melting and solidification, respectively, and p_M, p_S are probabilities given by:

$$p_{M,S} = f_{M,S} \cdot A_{M,S} \tag{2.28}$$

Here $f_{M,S}$ is the probability that an atom of sufficient energy is moving toward the interface, and $A_{M,S}$ is the probability that an atom is not kicked back by an elastic collision upon arrival.

At equilibrium, the flux of atoms toward and away from the interface must be equal, that is, $(dn/dt)_M = (dn/dt)_S$. Thus, the two curves must intersect at T_e (Fig. 2.12). For solidification to occur, more atoms must jump from L to S than from S to L. Consequently, the solidifying interface must be at lower temperature than T_e by an amount that is called as *kinetic undercooling* , ΔT_k.

Another approach to this problem (e.g., Biloni and Boettinger 1996) would be to consider that the overall solidification velocity is simply:

$$V = \text{Rate of solidification} - \text{Rate of melting} = V_c - V_c \exp\left(-\Delta G / RT_i\right)$$

where ΔG is expressed in J/mole. V_c corresponds to the hypothetical maximum growth velocity at infinite driving force. Then, using series expansion for the exponential term ($1 - e^{-x} \approx x$), neglecting 2nd and higher order terms, and assuming that Eq. 2.10 is valid near equilibrium we obtain:

$$V = V_c \frac{\Delta H_f \Delta T_k}{RT_e^2} \quad \text{or} \quad \Delta T_k = \frac{RT_e^2}{\Delta H_f} \frac{V}{V_C} \tag{2.29}$$

Two hypotheses have been used to evaluate V_c. The first one (e.g., Turnbull 1962) assumes that the rate of forward movement (atoms incorporation in the solid) is the same as the rate at which atoms can diffuse in the melt. Thus, $V_c = D_L/a_o$, where a_o is the interatomic spacing. The second one, the so-called *collision limited growth model* (Turnbull and Bagley 1975), assumes that the solidification event may be

Table 2.1 Hierarchy of equilibrium. (Boettinger and Perepezko 1986)

Increasing undercooling or solidification velocity ⇓	I. Full diffusional (global) equilibrium
	A. No chemical potential gradients (composition of phases are uniform)
	B. No temperature gradients
	C. Lever rule applicable
	II. Local interfacial equilibrium
	A. Phase diagram gives compositions and temperatures only at liquid–solid interface
	B. Corrections made for interface curvature (Gibbs–Thomson effect)
	III. Metastable local interface equilibrium
	A. Stable phase cannot nucleate or grow sufficiently fast
	B. Metastable phase diagram (a true thermodynamic phase diagram missing the stable phase or phases) gives the interface conditions
	IV. Interface nonequilibrium
	A. Phase diagram fails to give temperature and compositions at the interface
	B. Chemical potentials are not equal at the interface
	C. Free energy functions of phases still lead to criteria for impossible reactions

limited only by the impingement rate of atoms with the crystal surface. Then $V_c = V_o$, where V_o is the speed of sound. Note that V_o is approximately three orders of magnitude higher than D_L/a_o. Experimental analysis of rapidly growing dendrites in pure melts (Coriell and Turnbull 1982) has confirmed the collision limited growth model. Typically, for metals the kinetic undercooling is of the order of 0.01–0.05 K.

2.3 Departure from Equilibrium

We have demonstrated that for solidification to occur a certain amount of undercooling is necessary. Solidification cannot occur at equilibrium. Depending of the amount of undercooling different degrees of departure from equilibrium may occur, following a well-defined hierarchy. As shown in Table 2.1, as the undercooling or the solidification velocity increases, the liquid-to-solid transformation changes from fully diffusional to nondiffusional.

Global equilibrium, (I), requires uniform chemical potentials and temperature across the system. Under such conditions, no changes occur with time. In solidification processing such conditions exist only when the solidification velocity is much smaller than the diffusion velocity. Such conditions truly exist only when solidification takes place over geological times (Biloni and Boettinger 1996), or after long time annealing (see Application 2.1). When global equilibrium exists, the fraction

of phases can be calculated with the lever rule, and the phase diagram gives the uniform composition of the liquid and solid phases.

During solidification of most castings, both temperature and composition gradients exist across the casting. Nevertheless, in most cases, the overall kinetics can be described with sufficient accuracy by using the mass, energy, and species transport equations to express the temperature and composition variation within each phase, and equilibrium phase diagrams to evaluate the temperature and composition of phase boundaries, such as the solid/liquid interface. This is the local equilibrium condition, (II). Most phase transformations, with the exception of massive (partitionless) and martensitic transformations can be described with the conditions present under (II).

Metastable equilibrium, (III), can also be used locally at the interface. The most common case is the gray-to-white (metastable-to-stable) transition in cast iron that occurs as the cooling rate increases. The stable eutectic graphite-austenite is gradually substituted by the metastable iron carbide-austenite because of difficulties in the nucleation of graphite and the higher growth velocity of the metastable eutectic. Metastable transformation can occur at solidification velocities exceeding 0.01 m/s. Usually, solidification occurring at rate above this value is termed rapid solidification.

For both stable and metastable local equilibrium, the chemical potentials of the components across the interface must be equal for the liquid and for the solid. However, at large undercooling, achieved for example when using high-solidification velocities, this condition ceases to be obeyed. The solidification velocity exceeds the diffusive speed of solute atoms in the liquid phase. The solute is trapped into the solid at levels exceeding the equilibrium solubility. These conditions, (IV), correspond to rapid solidification. Typically, for solute trapping to occur, the solidification velocity must exceed 5 m/s (Boettinger and Coriell 1986).

The preceding analysis is useful in attempting to classify practical solidification processes based on the degree of equilibrium at which they occur as follows:

- Processes occurring with local interface equilibrium : shape casting, continuous casting, ingot casting, welding (arc, resistance), directional solidification.
- Processes occurring with interface nonequilibrium : welding (laser), melt spinning, atomization, surface remelting.

2.3.1 Local Interface Equilibrium

For the time scale (cooling rates) typical for solidification of castings, the assumption of local interface equilibrium holds very well. However, the interface temperature is not only a function of composition alone, as implied by the phase diagram. Interface curvature, as well as heat and solute diffusion, affects local undercooling. Accordingly, to express the condition for local equilibrium at the S/L interface all

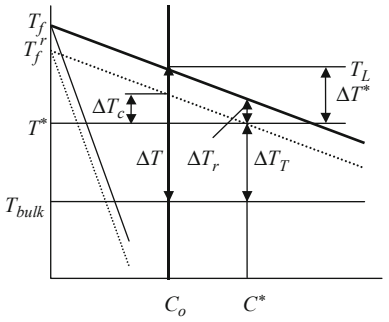

Fig. 2.13 The various components of interface undercooling with respect to the bulk temperature under the condition of local interface equilibrium

the contributions to the interface undercooling must be considered. The total undercooling at the interface with respect to the bulk temperature, T_{bulk}, is made of the algebraic sum of all the undercoolings previously derived (see Fig. 2.13):

$$\Delta T = \Delta T_k + \Delta T_r + \Delta T_c + \Delta T_T + \Delta T_P \tag{2.30}$$

Ignoring the kinetic and pressure undercooling, and since $T_L = T_f + m\,C_o$, the interface undercooling under the condition of local equilibrium for castings solidification can be written as:

$$\begin{aligned} \Delta T = \Delta T_T + \Delta T_c + \Delta T_r &= (T^* - T_{bulk}) + (T_L - T^*) + \Gamma K \\ &= T_f + mC_o + \Gamma K - T_{bulk} \end{aligned} \tag{2.31}$$

where T_f is the melting point of the pure metal (see Application 2.2).

In practical metallurgy, the solidification velocity is increased by increasing the cooling rate. As the cooling rate increases the length scale of the microstructure (e.g., dendrite arm spacing (DAS)) decreases. For cooling rates up to 10^3 K/s, local equilibrium with compositional partitioning between the liquid and solid phases at the solidification interface is maintained. The interface undercooling is small. However, when the cooling rate increases above 10^3 K/s nonequilibrium solidification occurs.

Local equilibrium can occur even at significant undercooling under the equilibrium temperature if nucleation is avoided. In this case, the liquidus and solidus lines can be extended as metastable lines, as shown in Fig. 2.14.

2.3.2 Interface Nonequilibrium

It has been shown that for a multiphase system a condition for equilibrium is that the chemical potential of each component must be the same in all phases, as stated by Eq. 2.4. This is shown graphically in Fig. 2.15. It is noticed that, while the chemical potentials in the liquid and solid are equal, the compositions are not. The necessary

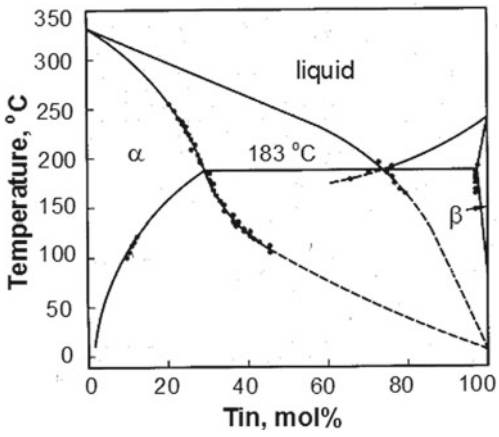

Fig. 2.14 The stable Pb–Sn phase diagram (*solid line*) with superimposed calculated metastable extensions (*dotted lines*) of the liquidus and solidus lines, and measured data. (Fecht and Perepezko 1989)

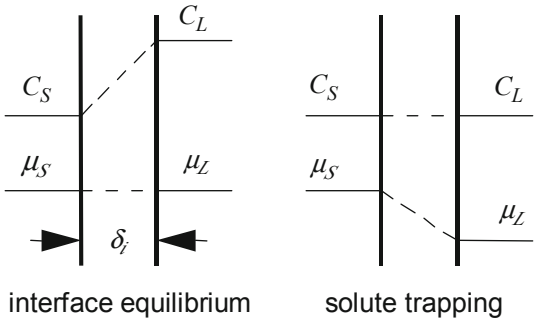

Fig. 2.15 Interface composition and chemical potential for equilibrium and diffusionless solidification (*solute trapping*)

condition for interface equilibrium is $V << D_i/\delta_i$, where V is the solidification velocity, D_i is the interfacial diffusion coefficient, and δ_i is the atomic jump distance. Note that D_i is smaller than the bulk liquid diffusion coefficient, D_L. The equilibrium partition coefficient is calculated from the phase diagram with Eq. 2.19. If the ratio between the two velocities is reversed, that is $V >> D_i/\delta_i$, as shown in Fig. 2.15, the equality between the chemical potentials is lost, but the composition becomes uniform across the interface. The partition coefficient becomes one. Solute trapping occurs. Using the typical values of $D_i = 2.5\ 10^{-9}$ m^2/s and $\delta_i = 0.5\ 10^{-9}$ m, the critical velocity for solute trapping is calculated to be 5 m/s.

For solute trapping to occur, the interface temperature must be significantly undercooled with respect to T_L. During partitionless solidification ($C_S^* = C_L^*$), a thermodynamic temperature exists which is the highest interface temperature at which partitionless solidification can occur. This temperature is called the T_o temperature, and is the temperature at which the molar free energies of the solid and liquid phases are equal for the given composition. The locus of T_o over a range of compositions constitutes a T_o curve. The liquid and solid phase compositions are equal along the T_o curve.

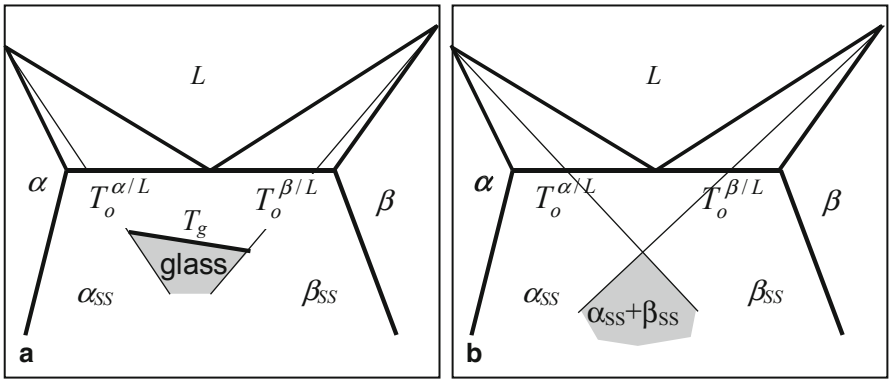

Fig. 2.16 Schematic representation of T_o curves for two different eutectic systems. (Perepezko and Boettinger 1983)

Some examples of such curves are given in Fig. 2.16. They can be used to evaluate the possibility of extension of solubility by rapid melt quenching. If the T_o curves are steep (Fig. 2.16a), single phase α or β crystals with compositions beyond their respective T_o cannot form from the melt. The solidification temperature in the vicinity of the eutectic composition can be depressed to the point where an increased liquid viscosity stops crystallization (glass temperature transition, T_g). If the T_o curves are shallow (Fig. 2.16b), for composition below both T_o curves, a mixture of α and β crystals could form, each phase having the same composition as the liquid.

Baker and Cahn (1971) formulated the general interface condition for solidification of binary alloys by using two response functions:

$$T^* = T\left(V, C_L^*\right) - \Gamma K \tag{2.32}$$

$$C_S^* = C_L^* k^*(V, C_L^*) \tag{2.33}$$

At zero-interface velocity (equilibrium), the functions T and k^* are directly related to the phase diagram. Indeed, $T(0, C_L^*)$ describes the liquidus temperature of the phase diagram and $k^*(0, C_L^*)$ is the equation for the equilibrium partition coefficient, Eq. 2.19. The dependence of k^* on interface curvature is ignored.

Several models have been proposed to describe the dependence of the partition coefficient on velocity. The most widely accepted is the one proposed by Aziz (1982). Ignoring the composition dependence of the partition coefficient, its functional dependence for continuous growth is:

$$k^*(V) = \frac{k_e + \delta_i \cdot V/D_i}{1 + \delta_i \cdot V/D_i} \tag{2.34}$$

where k_e is the equilibrium partition coefficient.

Note that for $V = 0$, $k^* = k_e$, and for very large V, $k^* = 1$. D_i is unknown. In some other models liquid diffusivity rather than interfacial diffusivity is used. The atomic diffusion speed $V_i = D_i/\delta_i$, is usually obtained by fitting Eq. 2.34 to experimental curves showing velocity dependence on partition coefficients. Some typical values for V_i are 17 m/s for Sn (Hoaglund et al. 1991), 33 m/s for Ni-0.6 at% C (Barth et al. 1999), and 5 m/s for Ag-5at% Cu (Boettinger and Coriell 1986). From this analysis it follows that for solute trapping to occur two conditions are necessary: $k^* = 1$ and $T^* < T_o$.

By evaluating the change in free energy and assuming a linear kinetic law for the interface velocity (from Eq. 2.29), Baker and Cahn (1971) calculated the two response functions for a flat interface to be:

$$T^* = T_f + m_L(V)C_L^* + \frac{m_L}{1-k_e}\frac{V}{V_o} \text{with} m_L(V) = \frac{m_L}{1-k_e}\left[1 - k^*\left(1 - \ln\frac{k^*}{k_e}\right)\right] \tag{2.35}$$

$$C_S^* = k^* C_L^* \tag{2.36}$$

Boettinger and Coriell (1986) have proposed a slightly different derivation, substituting the last term in Eq. 2.35 for interface temperature with the kinetic undercooling given by Eq. 2.29, to obtain:

$$T^* = T_f + m_L(V)C_L^* - \frac{RT_e^2}{\Delta H_f}\frac{V}{V_o} \tag{2.37}$$

Note that if $D_i/\delta_i = 0$ and $V_o = \infty$, then the conditions for local interface equilibrium revert to the equations previously introduced:

$$T^* = T_f + m_L C_L^* \text{and} C_S^* = k_e C_L^* \tag{2.38}$$

2.4 Applications

Application 2.1 Calculate the time required for the directional solidification of a rod having the length $l = 10$ cm, so that full diffusional equilibrium operates during solidification.

Answer Assume $D_L = 10^{-9}$ m/s. For equilibrium solidification to occur diffusion will have to go to completion; that is the solute should be able to diffuse over the entire length of the specimen. The diffusion velocity for complete diffusion over the sample of length l is $D_L/l = 10^{-9}/10^{-2} = 10^{-7}$ m/s. The solidification velocity must be much smaller than the diffusion velocity, i.e., $V_S << D_L/l$. Assume $V_S = 10^{-10}$ m/s. Then, the solidification time is $t = l/V_S = 10^{-2}/10^{-10} = 10^8$ s = 3.17 years.

Application 2.2 Consider a Cu-10 %Sn bronze (phase diagram in Appendix C). Assume solidification with planar S/L interface under local equilibrium conditions. A thermocouple placed far from the interface reads 950 °C. What is the interface undercooling at the beginning of solidification? Calculate the change in interface undercooling when the average (bulk) composition has changed from 10 to 12 %.

Answer The interface undercooling is given by Eq. 2.31. The contribution of curvature is ignored as the interface is planar. From the phase diagram $T_f = 1085\,°C$. The liquidus slope can be calculated using values at the temperature of 798 °C, as follows: $m = \Delta T/\Delta C = (1085 - 798)/(-26) = -11$. C_o is given as 10 %. Substituting in Eq. 2.31 we obtain the initial interface undercooling to be $\Delta T = 25\,°C$.

The change in interface undercooling when the bulk composition increases to 12 % is simply $m\,(C_o - C_{bulk}) = -11(10 - 12) = 22°C$.

References

Aziz MJ (1982) J. Appl. Phys. 53:1158

Baker JC, Cahn JW (1971) in: Solidification. ASM Metals Park, OH, p 23

Barth M, Holland-Moritz D, Herlach DM, Matson DM, Flemings MC (1999) in: Hofmeister WH et al. (eds) Solidification 1999. The Minerals, Metals and Materials Soc., Warrendale PA, p 83

Biloni H, Boettinger WJ (1996) Solidification. In: Cahn RW, Haasen P (eds) Physical Metallurgy. Elsevier Science BV, p 670

Boettinger WJ, Perepezko JH (1985) in: Das SK, Kear BH, Adam CM (eds) Rapidly Solidified Crystalline Alloys. The Metallurgical Soc., Warrendale PA, p .21

Boettinger WJ, Coriell SR (1986) in: Sahm PR, Jones H, Adams CM (eds) Science and Technology of the Supercooled Melt. NATO ASI Series E-No. 114, Martinus Nijhoff, Dordrecht, p 81

Chalmers B (1956) Trans. AIME 200:519

Coriell SR, Turnbull D (1982) Acta metall. 30:2135

Fecht HC, Perepezko JH (1989) Metall. Trans. 20A:785

Fredriksson H, Åkerlind U (2012) Solidification and Crystallization in Metals and Alloys. Wiley

Hoaglund DE, Aziz MJ, Stiffer SR, Thomson MO, Tsao JY, Peercy PS (1991) J. Cryst. Growth 109:107

Perepezko J H, Boettinger WJ (1983) Mat. Res. Soc. Symp. Proc. 19:223

Sobczak JJ, Drenchev L, Asthana R (2012) Int. J. Cast Metals Res. 25(1):1

Turnbull D (1962) J. Phys. Chem. 66:609

Turnbull D, Bagley BG (1975) in: Hannay NB (ed) Treatise on Solid State Chemistry. Plenum, NY, 5:513

Verhoeven JD (1975) Fundamentals of Physical Metallurgy. John Wiley & Sons, New York, p 238

http://www.springer.com/978-3-319-15692-7

Science and Engineering of Casting Solidification
Stefanescu, D.
2015, XVI, 556 p. 300 illus., 100 illus. in color.,
Hardcover
ISBN: 978-3-319-15692-7